Astron. Astrophys. 320, 575–579 (1997)

ASTRONOMY
AND
ASTROPHYSICS

CS chemistry in the bipolar nebula CRL 2688

T. Kasuga[1,2], **I. Yamamura**[3,4,5], **and S. Deguchi**[2]

[1] Department of Instrument and Control Engineering, Hosei University, Kajino 3-7-2, Koganei, Tokyo 184, Japan
[2] Nobeyama Radio Observatory, National Astronomical Observatory, Minamimaki, Minamisaku, Nagano 384-13, Japan
[3] Department of Astronomy, School of Science, University of Tokyo, Bunkyo, Tokyo 113, Japan
[4] Institute of Astronomy, Faculty of Science, University of Tokyo, Osawa 2-21-1 Mitaka, Tokyo 181, Japan
[5] temporary address: SRON Laboratory for Space Research Groningen, P. O. Box 800, 9700 AV Groningen, The Netherlands

Received 21 May 1996 / Accepted 17 September 1996

Abstract. High spatial-resolution observations of the protoplanetary nebula CRL2688 were made by the CS J =1–0 and J =2–1 lines with the Nobeyama Millimeter Array with angular resolutions of $6''\times6''$ and $3''\times3''$, respectively. The mapping observations reveal that strong CS peaks in the J =2–1 line are located symmetrically at both sides of the optical dark lane at the center, though the CS J =1–0 distribution is rather round. These CS peaks seem to be slightly misaligned from the optical bipolar axis. A modeling of the CRL 2688 envelope results that the density distribution is nearly spherically symmetric but the abundance of CS is enhanced near the polar regions. The increase of the CS abundance near the poles can be explained by the chemistry of sulfur containing molecules in the postshocked region in the high-velocity flow.

Key words: stars: CRL 2688 – stars: AGB, post-AGB – stars: mass loss – circumstellar matter – radio lines: stars

1. Introduction

The infrared source, CRL 2688, is a reflection nebula (the "Egg Nebula") with remarkably symmetric optical lobes which are separated by dark lane (Ney et al.1975). The Hubble Space Telescope found search-light beams and multiple arclets in this source (Sahai et al. 1995). The central object is an evolved star with a spectral type of F5 (Crampton et al. 1975). Radio line observations revealed that the circumstellar envelope consists of rich carbon-bearing molecules (Zuckerman et al. 1976; Nguyen-Q-Rieu et al. 1988). High-resolution radio observations found a weak bipolarity in the high-velocity molecular outflow (Heiligman et al 1986), or an longated feature along the optical dark lane. (Kawabe et al. 1987, Bieging & Nguyen-Q-Rieu 1988). The overall distribution of CO emission is, however, found to be rather spherically symmetric (Truong-Bach et al. 1990). The high velocity components of about 20-30 km s^{-1} of ^{13}CO are not oriented along the the bipolar axis (Yamamura et al. 1995, 1996). It has been believed that the CS molecule is a good probe for the dense disk in young stellar objects (e. g., Kaifu et al. 1983). However, in the evolved objects, a potential of the CS molecule as a disk probe is still unknown. The mapping observation of the CS J =2–1 line for the alternative protoplanetary object, CRL 618, has shown that emission is not necessarily associated with the disk (Hajian et al. 1995). To study the CS distribution for the representative protoplanetary nebula CRL 2688, we have made high spatial-resolution observations.

Send offprint requests to: S. Deguchi[2]; deguchi@nro.nao.ac.jp

2. Observations

Observations by the CS J =1–0 and J =2–1 transitions at 48.991 and 97.981 GHz, respectively, were made with Nobeyama Millimeter Array during the Dec. 1988 – April 1989 session using five antennas with 2 configurations in each CS line (20 base lines each). The SIS receivers at 49 and 98 GHz were operated in the double side band mode and the system temperatures at these frequencies were about 300–400 K. The side-band separation was made with a phase switching by 90 degree. The 1024 channel, digital FFT spectro-correlator with a band width of 320 MHz was used, giving the velocity resolution of 1.9 and 0.9 km s^{-1} per channel for the J =1–0 and 2–1 transitions, respectively. The radio source, BL Lac (2200+420), was used as a flux and phase calibrator. The flux density of the calibrator at each frequency was obtained by observing Venus and Mars at each configuration. The flux densities of 3.7 and 2.2 Jy at 49 and 98 GHz, respectively, were adopted through the observing session. The band pass calibrations were made by observing 3C84 after every CRL 2688 observation. The data were reduced using the Nobeyama package of the AIPS system and CLEANed maps were made. The resulting synthesized beam was nearly circular with a full width of a half maximum of $6''$ at 49 GHz and $3''$ at 98 GHz. The continuum was detected only at 98 GHz and the total flux density of the continuum was 0.15 Jy at 98 GHz,

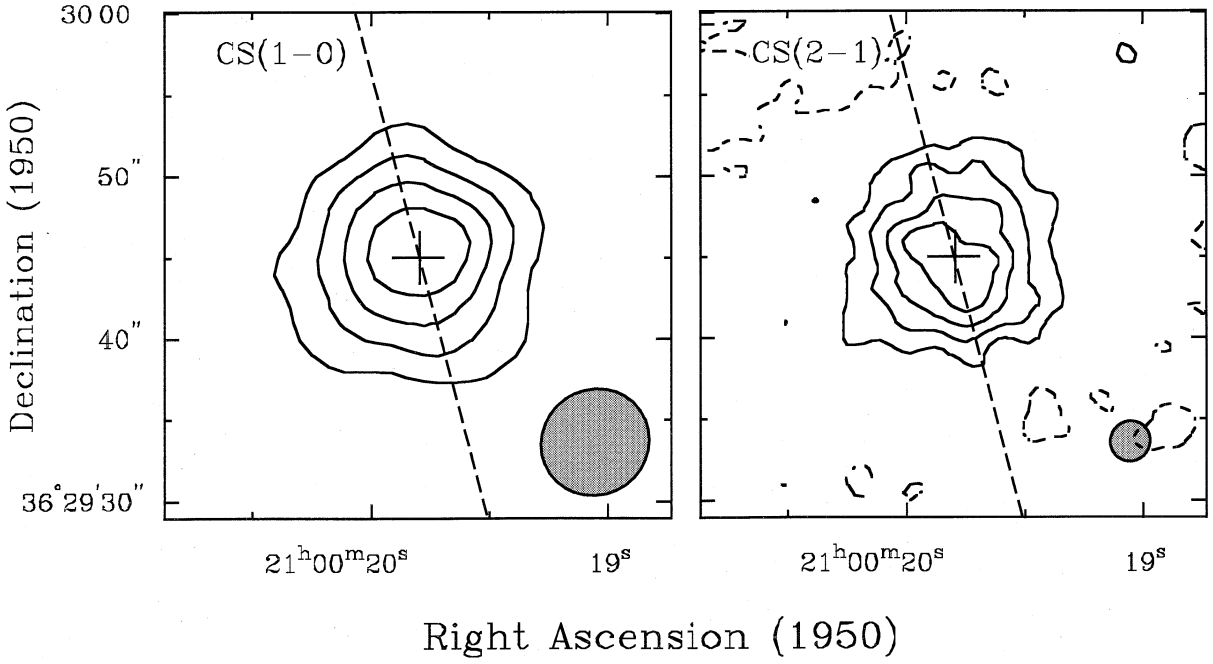

Fig. 1. The integrated-intensity maps of the CS J =1–0 (right pannel) and$J$ =2–1 (left pannel) lines for CRL 2688. The CS emission is integrated in the velocity range between V_{lsr} =-80 and -15 km s^{-1}. Contour leves are drawn in every 20 percent of the peak value. The broken lines shows a direction of the optical bipolar axis. The gray ellipse near the bottom-right corner shows a beam shape. The cross mark shows the peak of emission (RA =21h00m19.8s, $Decl.$ =36°29'45″, 1950).

which is consistent with previous measurements (Knapp et al. 1994).

Fig. 1 shows integrated intensity maps for the J =1–0 (left pannel) and J =2–1 (right pannel) lines. Emission is extended by about 15″. They are approximately circular for both lines, but slight deviation from the circular symmetry can be seen in the central part in the right pannel (the J=2–1 line). The elongated structure can be seen in the J =2–1 map. The direction of elongation seems to be misoriented from the direction of the optical bipolar axis which is shown as the broken line in figure 1. It is possible that the complex structure seen in the J =2–1 map is smeared with the larger beam in the J =1–0 map and becomes unrecognizable.

Figs. 2 and 3 show the resulting channel maps of the CS J =1–0 and 2–1 lines of CRL 2688. The J =1–0 maps (Fig. 2) with a 6″ resolution show that emission is almost peaked at the center, i.e., at the mid point between the optical bipolar lobes. In contrast, the J =2–1 maps (Fig. 3) with a 3″ resolution show rather complicated structure. The total flux densities of the J =1–0 and 2–1 lines at the peak (calculated from the map) are 1.1 and 4.5 Jy, respectively.

The most distinctive features in the J =2–1 channel maps are two concentrations of emission at the North-East and South-West sides of the core. The two peaks of emission are separated by about 5″. They are closely oriented to the direction of the optical bipolar axis (NNE to SSW), but look slightly misaligned to the bipolar axis. Another notable feature is a lateral elongation which is oriented approximately in the direction of the optical dark lane; this feature can be seen in the panels (j), (l), and (m) in Fig. 3.

The line profile which is integrated over the source is shown in Fig. 4. The high velocity component at V_{lsr} = -70 to -55 km s^{-1} seems to be detected, though it is quite difficult to recognize it in the indivisual channel maps. The peak flux density of 4.5 Jy of the J =2–1 line is consistent with the previous single-dish observation of T_B = 0.12 K of this transition with the NRAO 11-m telescope (Zuckerman et al. 1976) and the missing flux is estimated to be less than 20% in the present interferometric observations.

3. Discussion

To obtain physical parameters of the envelope of CRL 2688, we have calculated the CS line intensities with the Large-Velocity-Gradient(LVG) approximation. In the modeling based on ^{13}CO interferometric observations (Yamamura et al. 1996), we calculated the gas density in the envelope of CRL 2688 under a given temperature distribution. The result was that the density distribution is roughly spherically symmetric in this source. In this model, the high-velocity component is present at the part of the core of radius of $\sim 3 \times 10^{16}$ cm. However, it is clear that the spherically symmetric model cannot reproduce the doubly peaked morphology in the observed CS maps.

For a new model to be consistent with the previous model based on the ^{13}CO observations, we introduce the model in which the CS abundance is enhanced at the narrow postshocked regions located at the inner core. Overall density and kinetic

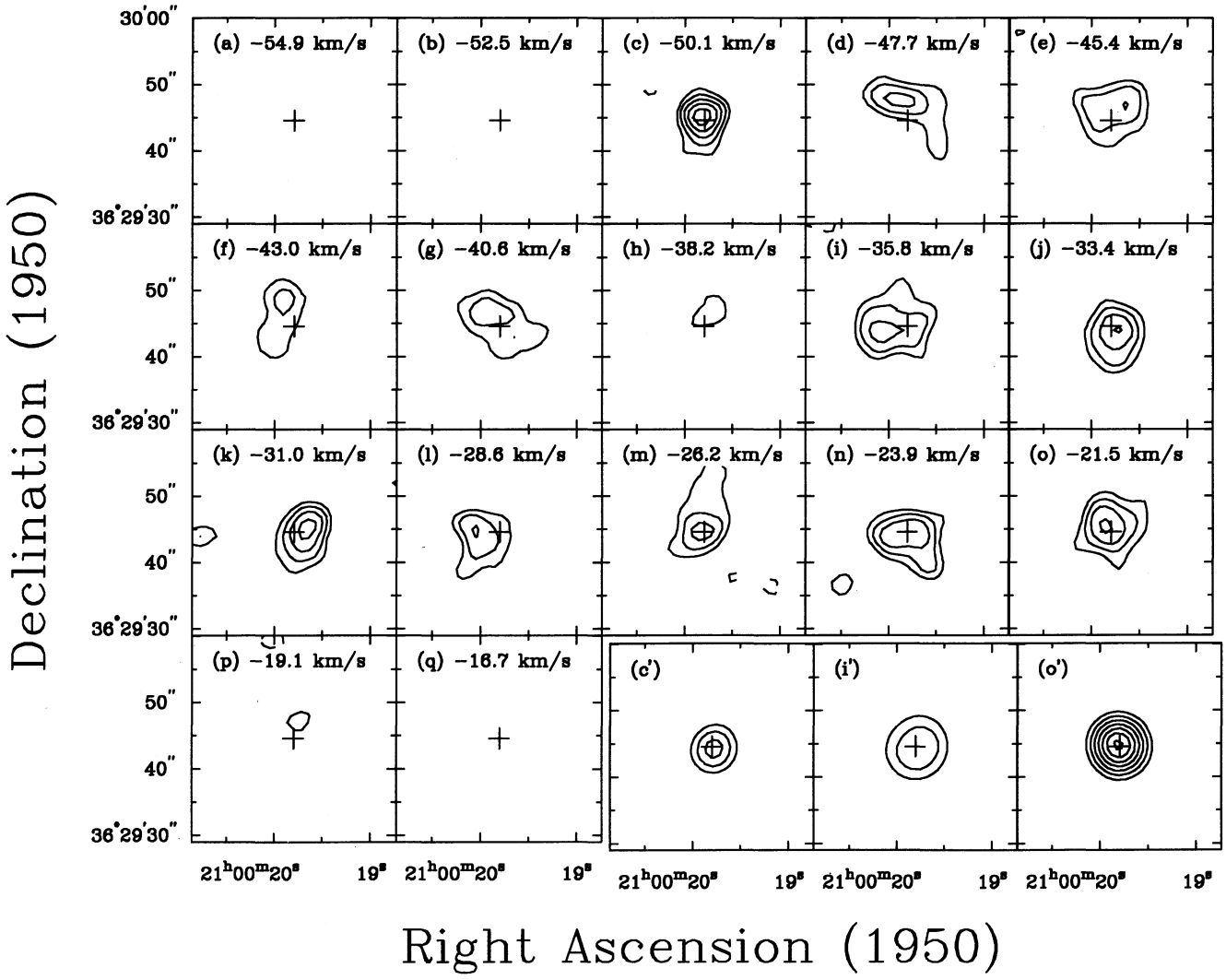

Fig. 2a–o'. The velocity-channel maps of the J =1–0 line for CRL 2688. Contour leves are drawn in every of 90 mJy/beam (one sigma) above the lowest contour level (three sigma). The bottom-right three panels, (c'), (i'), and (o'), are the channel maps otained from the model calculations. The cross mark indicate the peak position of emission

temperature distributions in the outer envelope are taken to be the same as used in the ^{13}CO modeling and the CS abundace is constant in the outer envelope. The postshocked regions are located near the center within a few arcsec. The shock is considered to propagate in narrow cones from the central star in the two opposite directions, reaching now at the radius r_s from the center. For simplicity, we assume that the postshocked regions are represented by two oppositely placed frustums of narrow cones (for geometry, see Fig. 13 of Yamamura et al. 1996) and that the CS abundance is uniform in the frustums. The axis of the narrow cone is taken to be rotated by 45 degree from the north (slightly misoriented from the bipolar axis). The top and bottom of the frustum of cone are taken to be located at radii, r_i and r_s, from the central star. The CS abundance, an opening angle of the cone, and gas kinetic temperature in frustums of the cone are taken as free parameters and to be adjusted to fit the calculated to the observed intensity of the doubly peaked feature of CS emission. The gas density is given by the assumption of the constant mass loss rate of 3.0×10^{-4} M$_\odot$ yr^{-1} for both inside and outside of the cone (Yamamura et al. 1996).

The rate equations are numerically solved under the LVG approximation. The level populations of CS up to J =12 are calculated and intensities at each position and at each frequency are multiplied by the beam factor and converted to the flux densities in velocity channel maps. They are compared with the observed channel maps. The calculated channel maps are shown on the three separated panels at the bottom right in Figs. 2 and 3. The best-fit parameters of the model are shown in Table 1. The model correctly reproduces the singly and the doubly peaked distributions in the the J =1–0 and J =2–1 channel maps and the peak fluxes of both J =1–0 and 2–1 lines in the model are consistent with the observational values (see also Fig. 4). The excitation temperature of the CS J =1–0 and 2–1 lines in the model is about 10 K at the outer envelope and at about 40 K in the cone.

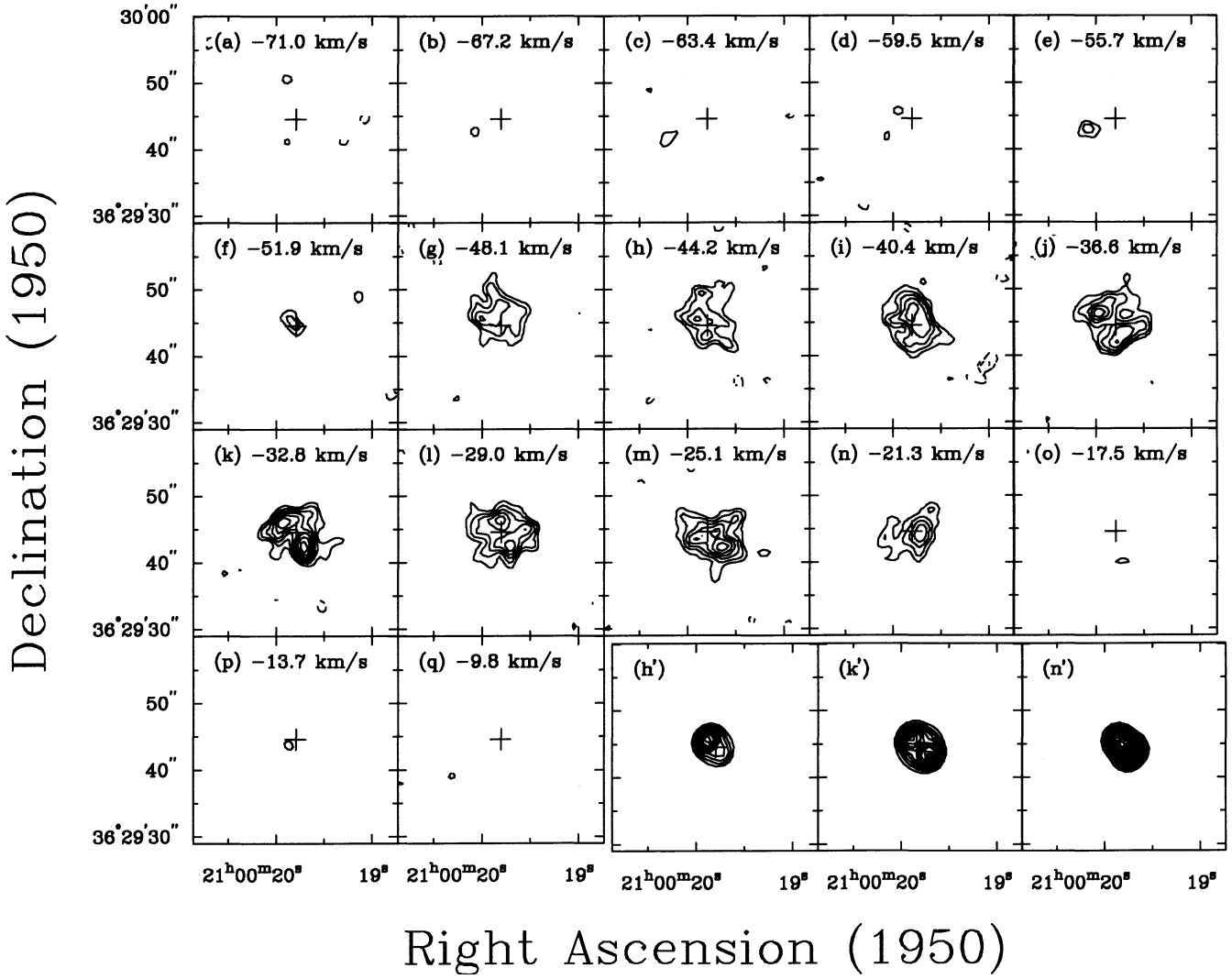

Fig. 3a–n'. The velocity-channel maps of the J =2–1 line for CRL 2688. The contour levels are drawn in every 50mJy/beam (one sigma) above the lowest contour level (three sigma). The bottom-right three panels, (g'), (k'), and (n'), are the channel maps obtained from the model calculations.

The CS abundance in the postshocked region, 9×10^{-7} per H_2, which is obtained in this paper is by about a factor of few smaller than the value obtained by the previous single-dish observations in the J =3–2, and 5–4 transitions (Bujarrabal et al. 1994). This is because the previous model assumed the mass loss rate by a factor of 3 smaller than used in this paper and the distribution of CS was uniform in the envelope. In addition, we use a higher kinetic temperature in the cone. The overall abundance of CS as 1.8×10^{-7} is consistent with the LTE atmospheric abundance in carbon stars (Lafont et al. 1982).

The increase of the CS abundance in the postshocked region can be explained by a shock chemistry. Based on time-dependent kinetic calculations, Mitchell (1984) demonstrated that the abundance of sulfur-containing molecules increases at postshock region. In this scheme, the CS molecule is created by the reaction,

$$\mathrm{CH + S \longrightarrow CS + H}\ .$$

For the slow shock (V =$\sim$ 7 km s^{-1}), the CS abundance is enhanced by about two orders of magnitude at postshocked region. The higher-velocity shock gives a lower CS abundance. This picture of shock chemistry seems to fit well to the present observations. The presence of emission of high J transitions for CO and CS (Jaminet et al. 1992, Bujarrabal et al. 1994) strengthens this idea. Moreover, the high abundance of complex radicals as C_2H and C_4H (Fukasaku et al. 1994) may indicate that the carbon chain molecules are dissociated in the shocked region.

The emission peaks of the J =2–1 line are not aligned in the direction of the optical bipolar axis (see the HST picture taken by Sahai et al. 1995), but rather in the direction close to the line connecting the center positions of the ^{13}CO high-velocity flow (Yamamura et al. 1995). It is possible that the positions of the shock are not on the bipolar axis but at slightly different locations . Mapping observations of near-infrared H_2 lines revealed quadra-polar components which are oriented along and perpen-

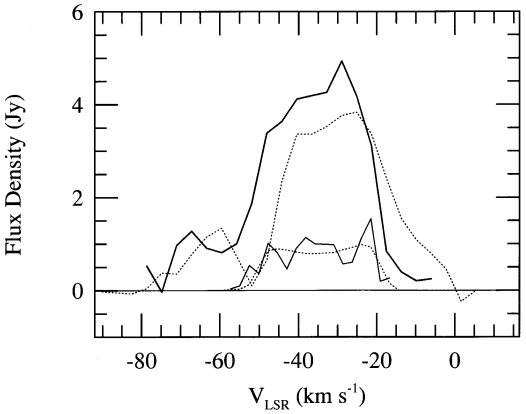

Fig. 4. Synthesized spectra of the CS J =1–0 and J =2–1 lines for CRL 2688. The top thick line shows the J =2–1 line and the lower thin line the J =1–0 line. Broken lines show the spectra calculated from the model.

dicular to the optical bipolar axis. (Latter et al. 1993, Skinner et al. 1996).

In contrast to CS, the other high-density tracers as HCN (Bieging & Rieu 1996), $H^{13}CN$, HNC, HC_3N, and SiS (Nguyen-Q-Rieu and Bieging 1990) exhibit an feature elongated in the direction perpendicular to the optical bipolar axis in CRL 2688. The CS J = 2–1 maps (Hajian et al. 1995) in CRL 618 does not exhibit any paticular sign of the shock enhancement of CS in the envelope but rather a clumpy structure which is similar to the structure found in CO (Shibata et al. 1993). It seems quite difficult to interpret all these observations consistently with a simple model. Models with clumpy or multiple-shell structures, may be necessary to explaine these observations. Higher spatial-resolution observations are definitely required to resolve complex morphological and kinematical structures of these sources.

4. Conclusion

In this paper, we have made high spatial-resolution observations of CS in the protoplanetary nebula CRL 2688. CS emission (the J =2–1 transition) is found to be doubly peaked at the core region and the direction of the peaks are misaligned to the bipolar axis. From these findings, we suspect that the CS abundance is enhanced in the postshocked region. CS molecules can be used as a probe for the shock chemistry in the protoplanetary nebulae.

Acknowledgements. The authors thank to the NRO interferometer group for operation of the Nobeyama Millimeter Array. I. Y. aknowledges a financial support by the Research Fellowship of Japan Society for the Promotion of Sciences.

Table 1. Model Parameters

Parameter	$value$
— Overall parameter —	
Inner radius (r_i)	$8 \times 10^{15}\ cm$
Outer radius (r_o)	$1 \times 10^{17}\ cm$
Mass-loss rate	$3.0 \times 10^{-4}\ M_\odot yr^{-1}$
Velocity ($r_i < r < r_o$)	$19.6\,(r/r_o)^{0.33}\ km\ s^{-1}$
Kinetic temperature (T_k)	$65(r/r_i)^{0.477}\ K$
CS abundance	$1.8 \times 10^{-7}\ perH_2$
— Parameter in the cone —	
Shock radius (r_s)	$6 \times 10^{16}\ cm$
Inner radius (r_i)	$8 \times 10^{15}\ cm$
Opening angle of the cone	45°
Velocity ($r_i < r < r_s$)	$40km\ s^{-1}$
Kinetic temparature	$2 \times T_k$
CS abundance	$9 \times 10^{-7}\ perH_2$

References

Bieging, J. H., Nguyen-Quang-Rieu, 1988, ApJ, 324, 516
Bieging, J. H., Nguyen-Quang-Rieu, 1996, AJ, 112, 706
Bujarrabal, V., Fuente, A., Omont, A., 1994, A&A, 285, 247
Crampton, D., Cowley, A. P., Humphreys, R. M., 1975, ApJL, 198, L135
Fukasaku, S., Hirahara, Y., Masuda, A., Kawaguchi, K., Ishikawa, S., Kaifu, N., Irvine, W. M., 1994, ApJ, 437, 410
Hajian, A.R., Phillips, J.A., & Terzian, Y., 1995, ApJ, 446, 244
Heiligman, G. M. et al., 1986, ApJ, 308, 306
Jaminet, P. A., Danchi, W. C., Sandell, G., Sutton, E. C., 1992, ApJ, 400, 535
Kaifu, N., et al., 1984, A&A, 134, 7
Kawabe, R., et al., 1987, ApJ, 314, 322
Knapp, G. R., Bowers, P. F., Young, K., Phillips, T. G., 1994, ApJL, 429, L33
Latter, W. B., Hora, J. L., Kelly, D. M., Deutsch, L. K., Maloney, P. R., 1993, AJ, 106, 260
Mitchell, G. F., 1984, ApJ, 287, 665
Ney, E. P., Merrill, K. M., Becklin, E. E., Neugebauer, G., Wynn-Williams, C. G., 1975, ApJL, 198, L129
Nguyen-Q-Rieu, Bieging, J. H., 1990, ApJ, 359, 131
Nguyen-Q-Rieu, Deguchi, S., Izumiura, H., Kaifu, N., Ohishi, M., Suzuki, H., and Ukita, N., 1988, ApJ, 330, 374
Sahai, R., Trauger, J., Evans, R. W., the WFPC2 IDT, 1995, BAAS, 27, 1344
Skinner, C. J. et al., 1996, A&A, submitted.
Shibata, K. M., Deguchi, S., Hirano, N., Kameya, O., & Tamura, S., 1993, ApJ, 415, 708
Truong-Bach, Nguyen-Q-Rieu, Morris, D., Deguchi, S., 1990, A&A, 230, 431
Yamamura, I., Onaka, T., Kamijo, F., Deguchi, S., Ukita, N., 1995, ApJL, 439, L13
Yamamura, I., Onaka, T., Kamijo, F., Deguchi, S., Ukita, N., 1996, ApJ, 465, 926
Young, K., Serabyn, G., Phillips, T. G., Knapp, G. R., Güsten, R., Schulz, A., 1992, ApJ, 385, 265
Zuckerman, B., Gilra, D. P., Turner, B. E., Morris, M., Palmer, P., 1976, ApJL, 205, L15

This article was processed by the author using Springer-Verlag LaTeX A&A style file *L-AA* version 3.